AEM
Journals.ASM.org

Genome Sequence of Thermotolerant *Bacillus methanolicus*: Features and Regulation Related to Methylotrophy and Production of L-Lysine and L-Glutamate from Methanol

Tonje M. B. Heggeset,[a] Anne Krog,[a,b] Simone Balzer,[a,b] Alexander Wentzel,[a] Trond E. Ellingsen,[a,b] and Trygve Brautaset[a]

SINTEF Materials and Chemistry, Department of Biotechnology, SINTEF, Trondheim, Norway,[a] and Norwegian University of Science and Technology, Department of Biotechnology, Trondheim, Norway[b]

Bacillus methanolicus **can utilize methanol as its sole carbon and energy source, and the scientific interest in this thermotolerant bacterium has focused largely on exploring its potential as a biocatalyst for the conversion of methanol into L-lysine and L-glutamate. We present here the genome sequences of the important *B. methanolicus* model strain MGA3 (ATCC 53907) and the alternative wild-type strain PB1 (NCIMB13113). The physiological diversity of these two strains was demonstrated by a comparative fed-batch methanol cultivation displaying highly different methanol consumption and respiration profiles, as well as major differences in their L-glutamate production levels (406 mmol liter^{-1} and 11 mmol liter^{-1}, respectively). Both genomes are small (ca 3.4 Mbp) compared to those of other related bacilli, and MGA3 has two plasmids (pBM19 and pBM69), while PB1 has only one (pBM20). In particular, we focus here on genes representing biochemical pathways for methanol oxidation and concomitant formaldehyde assimilation and dissimilation, the important phosphoenol pyruvate/pyruvate anaplerotic node, the tricarboxylic acid cycle including the glyoxylate pathway, and the biosynthetic pathways for L-lysine and L-glutamate. Several unique findings were made, including the discovery of three different methanol dehydrogenase genes in each of the two *B. methanolicus* strains, and the genomic analyses were accompanied by gene expression studies. Our results provide new insight into a number of peculiar physiological and metabolic traits of *B. methanolicus* and open up possibilities for system-level metabolic engineering of this bacterium for the production of amino acids and other useful compounds from methanol.**

Methylotrophic microorganisms can utilize one-carbon (C_1) sources, such as methane and methanol, as their sole sources for energy and biomass generation, and there exist a variety of different enzymes and pathways for C_1 metabolism among methylotrophs (14, 15). Bacteria that fix formaldehyde by the ribulose monophosphate (RuMP) pathway belong to three groups: Gram-negative obligate methylotrophs, Gram-positive facultative methylotrophs, and thermotolerant bacilli (3, 4, 19, 38). A number of Gram-positive thermotolerant bacilli with the ability to grow on methanol at temperatures up to 60°C have been isolated, and they were later collectively classified as *Bacillus methanolicus* (for a review, see reference 11). *B. methanolicus* is a so-called restricted methylotroph, which means that it can utilize few multicarbon sources for energy and growth. The scientific interest of these organisms has mainly been dedicated to exploring their potential as cell factories for industrial production of L-lysine and L-glutamate from methanol at elevated temperatures. *B. methanolicus* MGA3 (ATCC 53907) was isolated from soil samples in Minnesota (38), and it has been the major model strain used for metabolic engineering of this bacterium (9, 11, 27).

B. methanolicus has several additional unique traits, including (i) a novel NAD-dependent methanol dehydrogenase (MDH) for methanol oxidation (5, 18, 24), (ii) the ability to secrete up to 60 g liter^{-1} of L-glutamate (equal to 408 mmol liter^{-1}) in fed-batch methanol cultivation (9, 12), (iii) the ability to grow in cheap seawater-based media (29), and (iv) plasmid-dependent methylotrophy (10, 26). *B. methanolicus* MGA3 has a natural plasmid, pBM19, carrying *mdh* and five RuMP pathway genes, and the curing of pBM19 resulted in loss of the ability to grow on methanol. Methanol consumption by this organism involves the concerted recruitment of both plasmid and chromosomal genes, and this discovery represented the first documentation of plasmid-dependent methylotrophy (10, 26). Methanol oxidation is governed by MDH, which is catalytically activated by Act, a member of the Nudix hydrolase family (24, 28). A linear dissimilatory pathway for direct oxidation of formaldehyde to carbon dioxide has been documented based on ^{13}C nuclear magnetic resonance (NMR) data (35), but genetic evidence has been lacking.

Wild-type strains of *B. methanolicus* produce only about 0.2 g liter^{-1} L-lysine in fed-batch cultivation, while classical mutants secreting up to 47 g liter^{-1} of L-lysine (equal to 322 mmol liter^{-1}) have been selected (9, 11, 22). In recent years, several assumed key genes involved in L-lysine biosynthesis have been cloned, and functional expression tools have been developed. Recombinant *B. methanolicus* strains producing up to 11 g liter^{-1} of L-lysine have been constructed by manipulation with single genes representing the aspartate pathway (9, 27). We recently showed that multiple genes of the aspartate pathway can play important roles in L-lysine overproduction by *B. methanolicus* (32). Manipulation with enzymes representing the phosphoenol pyruvate (PEP) and pyruvate anaplerotic node and the entry into the tricarboxylic acid (TCA) cycle has indicated that the oxaloacetate (OAA) precursor supply is not a major bottleneck for L-lysine overproduction by *B.*

Received 14 March 2012 **Accepted** 7 May 2012
Published ahead of print 18 May 2012
Address correspondence to Trygve Brautaset, trygve.brautaset@sintef.no.

doi:10.1128/AEM.00703-12

methanolicus (9, 12). However, this has to be investigated further with additional relevant genes.

B. methanolicus MGA3 obviously represents a potentially interesting candidate for industrial production of L-glutamate from methanol. In addition, when the goal is to overproduce L-lysine, efficient modes to reduce unwanted L-glutamate production are desirable. Again, genetic insight into the L-glutamate biosynthetic and degradation pathways, as well as the transport capacities, is still lacking and represents a bottleneck for metabolic engineering, aiming at understanding, increasing, and controlling the L-glutamate production by this organism. We present here the genome sequences of *B. methanolicus* MGA3 and the physiologically very different alternative model strain PB1 (NCIMB13113). The genomes of a number of methylotrophic bacteria have been sequenced during recent years (for a review, see reference 15), and the present report represents the first genome sequences of methylotrophic bacteria belonging to the class of Gram-positive thermotolerant bacilli.

MATERIALS AND METHODS

Bacterial strains, growth media, and recombinant DNA procedures. *B. methanolicus* wild-type strains MGA3 (ATCC 53907) and PB1 (NCIMB13113) were generally grown in shake flasks at 50°C in 100 ml of $MeOH_{200}$ medium containing 200 mM methanol, in $Mann_{10}$ medium containing 20 g liter^{-1} mannitol, or in SOBsuc medium (26). When *B. methanolicus* strains were tested for their ability to grow on alternative C sources, cells were grown in $MeOH_{200}$ medium but with the methanol replaced with 2% (wt/vol) maltose, raffinose, ribose, fructose, sorbitol, or glucose. Amino acid content was analyzed as previously described (9). Standard recombinant DNA techniques were applied according to reference 37. *Escherichia coli* DH5α (Invitrogen) was used as the standard cloning host and was generally grown at 37°C in liquid or solid Luria-Bertani (LB) medium supplemented with ampicillin (0.2 g liter^{-1}) when appropriate. Plasmid DNA was isolated by the Wizard Plus SV Minipreps DNA Purification system (Promega), and linear DNA fragments were extracted from agarose gel slabs or PCR mixtures by the QIAquick gel extraction or PCR purification kit (Qiagen). DNA was amplified by the Expand High Fidelity PCR system (Roche), and routine DNA sequencing was performed by Eurofins MWG Operon.

Fed-batch methanol cultivation. Fed-batch methanol cultivation of *B. methanolicus* strains MGA3 and PB1 was performed in UMN1 medium containing 150 mM methanol, essentially as described before (27), using the following settings: the initial culture volume was 0.75 liter, and the inoculum was 70 ml divided by the optical density at 600 nm (OD_{600}) of the inoculum at the time of harvest (1.1 to 1.3). The initial and minimum agitation was 450 rpm, and the aeration rate was kept constant at 0.5 vol/vol/min. Agitation was controlled automatically to maintain a dissolved oxygen level of 30%. An automatic enrichment of oxygen up to 60% O_2 was applied once the agitation reached 1,300 rpm and continued in combination with the automatic control of agitation until the end of the cultivation, 50 h after inoculation. The initial use of 0.03% (vol/vol) Antifoam 204 (Sigma) and the supply of 4% Antifoam 204 in the methanol feed solution made further batch additions of antifoam agent dispensable during the cultivation. A conversion factor of 0.24 g liter^{-1} (dry weight) of cells per OD_{600} unit was used for determination of the dry weight of cells, and the OD_{600} range for collection of dry weight measurements of cells was between 18 and 53. The correction factors used for the determination of amino acid concentrations were between 1.15 and 1.4 for endpoint samples, based on the volume changes during the cultivation.

Preparation of total DNA and genome sequencing. Total DNA was isolated from exponentially growing *B. methanolicus* cells by phenol-chloroform-isoamyl alcohol (25:24:1) extraction and was dissolved in Tris-EDTA (TE) buffer. The quality and concentration of the DNA obtained were verified spectrophotometrically using a NanoDrop ND-1000 spectrophotometer and also by DNA gel electrophoresis. About 300 μl of MGA3 DNA with a concentration of 0.29 g liter^{-1} was shipped to 454 Life Sciences for pyrosequencing and draft sequence assembly, while 240 μl of PB1 DNA with a concentration of 0.163 g liter^{-1} was shipped to the Norwegian High-Throughput Sequencing Centre (www.sequencing.uio.no) for 8-kb paired-end GS FLX sequencing. The PB1 draft sequence assembly was built using Newbler at the freely available Bioportal computing service (www.bioportal.uio.no).

Sequence annotation and genome comparison. The draft MGA3 genome sequence, consisting of 87 large contigs (>500 bp), was submitted to the JCVI Annotation Service, where it was run through JCVI's prokaryotic annotation pipeline (www.jcvi.org/cms/research/projects/annotation-service/) and to the Bacterial Annotation System, BASys (http://basys.ca/basys/cgi/submit.pl) (40). A total of 120 large contigs (9 contigs of 517 to 3,068 bp were found to appear in 2 to 15 near-identical copies) were connected by the use of two different strategies. A total of 16 gaps were closed by connecting the coding sequences of partial genes located at contig ends, or of genes found at contig ends known to be colocalized. The remaining 94 gaps were connected using a primer walking strategy. All contig ends were inspected, and sites for the restriction enzymes EcoRI, BamHI, HindIII, PvuII, AgeI, AflIII, EcoRV, or XhoI were identified. MGA3 genomic DNA was individually digested with each of these enzymes, and the fragmented DNA was circularized by T4 DNA ligase. PCR fragments covering the individual contig ends were amplified from these circularized DNA fragments using primers that annealed close to the contig ends (oriented toward the unknown sequence) in addition to a primer that annealed close to the appropriate restriction site found within the ~1,000 bp from a contig end (oriented away from the end). The resulting PCR products were then submitted to sequencing directly (if shorter than 1.5 kb) or, alternatively, were subcloned into pGEM-T (Promega) before sequencing. All contig connections were verified by PCR amplification from a genomic template, followed by sequencing. The final genome consists of 10 large contigs and two plasmids and was resubmitted to the JCVI Annotation Service and to the NCBI Prokaryotic Genomes Automatic Annotation Pipeline (PGAAP) (www.ncbi.nlm.nih.gov/genomes/static/Pipeline.html) for final annotation. The PGAAP result formed the basis for the published GenBank data but was manually curated using BLAST (2) before submission.

The draft PB1 genome sequence, consisting of 82 large contigs organized in 3 scaffolds, was submitted to BASys and the RAST (Rapid Annotation using Subsystem Technology) Annotation server (http://rast.nmpdr.org/) for annotation (6). The scaffolds contained a total of 30 internal gaps, of which 28 were closed by PCR followed by sequencing. All the gaps turned out to contain highly repetitive sequences. The smallest scaffold, scaffold 3, consisted of one large (covering 18,763 bp) and one small (covering 1,424 bp) contig. The large contig covers the main part of the sequence known to represent the pBM19 plasmid in MGA3, while the small part was also found in two of the closed gaps and was later connected to the 5′ end of scaffold 2. Previous experiments have indicated that the PB1 strain contains a pBM19-like plasmid that is slightly larger than that in the MGA3 strain (10). Analysis using the Newbler contig graf viewer (data not shown) suggested that the scaffold 3 sequence is not found in a plasmid context but rather in two copies, interconnected with scaffold 2 and scaffold 1. PCR experiments succeeded in linking the 5′ ends of scaffold 2 with the small contig of scaffold 3; however, all attempts at connecting the large contig of scaffold 3 to scaffold 1 or 2 failed, as did attempts at closing the final gap in scaffold 1 (between contig 1 and contig 2) or the gap between the small and large contigs of scaffold 3. PCR experiments using either PB1 total DNA or isolated PB1 plasmid DNA as the template and primers annealing to the two ends of the large contig of scaffold 3 finally showed that both contigs of scaffold 3 are parts of a large, 20,187-bp plasmid (pBM20) but that the small contig is oriented in the inverse direction from that suggested by Newbler.

Microarray experimental design and microarray construction of strain MGA3. *B. methanolicus* MGA3 was grown methylotrophically on methanol and nonmethylotrophically on mannitol, and the gene expres-

sion profiles were compared. The experiment was performed in triplicate, from bacterial cultures grown on 3 different days. Custom gene expression microarrays for *B. methanolicus* (denoted MGA3_1) were designed with the help of eArray software (version 6.0; Agilent Technologies), according to the manufacturer's recommendations. Each customized microarray contained spots in quadruplicate, and the data set was duplicated, representing all the putative 3,641 coding sequences found in the initial draft sequence of *B. methanolicus* MGA3.

Isolation of total RNA, cDNA labeling, hybridization, and microarray scanning. Total RNA was isolated using the RNAqueous kit (Ambion). The quality of the RNA preparation was verified by an Agilent Bioanalyzer. Fluorescent Cy3-labeled cDNA was generated using the SuperScript indirect labeling system (Invitrogen), where CyDye fluorescent dyes (GE Healthcare Biosciences) were coupled to the amino allyl cDNA according to the manufacturer's instructions. Microarray hybridizations were carried out using the labeled cDNA together with the In Situ Hybridization Kit Plus (Agilent Technologies). Arrays were incubated at 65°C for 17 h in Agilent microarray hybridization chambers and were subsequently washed according to the Agilent protocol. The washed microarrays were scanned immediately in a DNA Microarray Scanner, model G2567AA (Agilent Technologies). The Feature Extraction software, version 9.5.1.1 (Agilent Technologies), was used for data extraction and quality control. The Agilent standard scenario for normalization was applied to all data sets. Extracted data were analyzed using the GeneSpring GX 10.0.2 software (Silicon Genetics). A 2-fold change (*P* value log ratio, <0.01) was used as the threshold for targeting genes differently expressed when grown methylotrophically versus nonmethylotrophically.

cDNA synthesis and qPCR. Quantitative PCR (qPCR) was used to compare the transcription levels of relevant *B. methanolicus* genes in cells growing methylotrophically on methanol with those in cells growing nonmethylotrophically on mannitol (26), and cDNA was synthesized using the First-Strand cDNA synthesis kit (Amersham Biosciences). qPCR analyses were performed using the ABI Prism 7700 sequence detection system with its default settings (Applied Biosystems) essentially as previously described (9). In brief, the qPCR primers were chosen with the assistance of the Primer Express 2.0 software (Applied Biosystems). The PCR mixture consisted of 12.5 μl of 2× SYBR Universal PCR Master Mix, 600 nM primers, 5 μl cDNA (0.25 g liter^{-1}), and H_2O to a final volume of 25 μl. Default cycling conditions were used. Relative quantification of the genes in question was done by normalizing the results, relative to 16S RNA (endogenous control) and a calibrator sample, using a comparative threshold cycle (C_T) method ($2^{-\Delta\Delta CT}$ method) according to the PE Applied Biosystems protocol (23, 30).

Primer pair sequences used were as follows: mdh2_f, 5′-GGATACATGTCAAACACTCAAAGTGC-3′; mdh2_r, 5′-TCTAGACACCATCGCATTTTTAATAATTTGG-3′; mdh3_f, 5′-GGATACATGTAAAACACTCAAAGTGC-3′; mdh3_r, 5′-TCTAGACACCATAGCATTTTTAATAATTTGGATG-3′; act_f, 5′-CCTGGTGCTGTAGCTGTAAT-3′; act_r, 5′-GCTTCGTCAAGTGTCAGTTC-3′; hps_f, 5′-GTAGCTGAGGTTCAGGAGTA-3′; hps_r, 5′-CTGCGATCATGTCAACAAGG-3′; phi_f, 5′-GAAGAAGCCGAAGCACTGGT-3′; phi_r, 5′-TGATCGTTACAGCCGCGATG-3′; pfk2_f, 5′-GTTACTGTTCTTGGCCATGTTCAG-3′; pfk2_r, 5′-TTGCAAGCACACGGTCAAA-3′; fba2_f, 5′-GCGAGAGGCGTTTCTGTTG-3′; fba2_r, 5′-CTGCGATTACGTCATCCTCTTG-3′; tkt2_f, 5′-ACGGTCATACACCTGGAGTTGA-3′; tkt2_r, 5′-CCATTCCAACTGCCATAGCA-3′; tal_f, 5′-GCCACCCGCAGCATGT-3′; tal_r, 5′-TGTAAGGCACAGTCGCAATATGA-3′; glpX2_f, 5′-CTGCAGTAGCGCTGAAATGC-3′; glpX2_r, 5′-GCATCATTTTGAGGCAAAAGC-3′; rpe2_f, 5′-CGGCGGAGTGAATAACGAAA-3′; rpe2_r, 5′-CGGCGGATCCTGCTACTAAC-3′; rpiB_f, 5′-GCCGGTTGCGGAAAAAGT-3′; rpiB_r, 5′-CGATACCTGTTCCGCAAATTAAG-3′; pgi_f, 5′-ACGGAACCAGCGATTGCA-3′; pgi_r, 5′-TTCGGATTTTCCGTAAATTGCTTCAGGAAA-3′; zwf1_f, 5′-GGAAACTGGAACGGTTTGCA-3′; zwf1_r, 5′-TATTGGCGTTGCACGAAGGCCA-3′; zwf2_f, 5′-CCACAATCATTTTCCGTTATTGG-3′; zwf2_r, 5′-CTAGGGCGAAGAGATTGGTCGGATAATGA-3′; pgl_f, 5′-TGAGTTAAAAGAAAAGAATTCCTTGTCA-3′; pgl_r, 5′-TAAAGCCGGGAAGCGGACCAAGA-3′; gnd_f, 5′-GCGAACATGGCATCCACTTTA-3′; gnd_r, 5′-CGGTACAGGAGTTTCCGGCGGG-3′; folD_f, 5′-ATGGGATCATGGTTTTACTTAAGGAA-3′; folD_r, 5′-GCTCCGCCCGATCACA-3′; fhs_f, 5′-TTGGCAAAAAGGCTATGATAGCT-3′; fhs_r, 5′-GCTCCTCCTTTTATTCCCATTGTT-3′; fdhA_f, 5′-GTATGGACCGTCGTTTTTTTCAC-3′; fdhA_r, 5′-CCAGCTGCAGAACAGATGGA-3′; fdhD_f, 5′-AGGATTTGCTTACGTGGATTTAGC-3′; fdhD_r, 5′-CAGCACGAGCCAATAAATCG-3′. The primer pair sequences of the pBM19 genes have been published previously (26).

Nucleotide accession numbers. The Whole Genome Shotgun projects have been deposited at DDBJ/EMBL/GenBank under accession numbers ADWW00000000 for MGA3 and AFEU00000000 for PB1. The versions described in this paper are the first versions, ADWW01000000 and AFEU01000000.

Microarray data accession number. The complete set of microarray data has been deposited in the Gene Expression Omnibus (GEO) database at the National Center for Biotechnology Information (http://www.ncbi.nlm.nih.gov/geo/) under the accession series GSE35298 (http://www.ncbi.nlm.nih.gov/geo/query/acc.cgi?acc=GSE35298).

RESULTS AND DISCUSSION

Fed-batch methanol cultivation displayed considerable physiological differences between the *B. methanolicus* wild-type strains MGA3 (ATCC 53907) and PB1 (NCIMB13113). We previously presented a total of 14 different wild-type isolates of *B. methanolicus* (10), and among these, MGA3 has been the major model strain used for metabolic engineering (9, 11, 12, 26, 27, 32). The majority of these strains—including MGA3—have been isolated from soil samples in the Minnesota area, while one strain, PB1, has been isolated from a sugar beet factory wastewater treatment system in Europe (20). We made a physiological comparison of the two *B. methanolicus* wild-type strains MGA3 and PB1 by analyzing both strains in fed-batch methanol cultivation. These two strains displayed fundamental differences with respect to growth, amino acid production, and respiration profiles (Fig. 1). The maximum biomass yield of PB1 is substantially lower than that of MGA3, and PB1 produces very little L-glutamate (11 mmol liter^{-1}) compared to MGA3 (406 mmol liter^{-1}). Also, the CO_2 evolution profiles of the two strains were highly different. Maximum L-lysine production levels were below 2 mmol liter^{-1} for both strains. Whether the observed differences in agitation between the two strains had any effect on these data remained unknown. The data for MGA3 were similar to analogous data presented previously under such conditions (12, 26), and together these data indicate physiological differences between these two wild-type strains. In order to generate a solid basis for understanding the similarities and differences in cell biology and physiology of *B. methanolicus* strains at a genome-scale level, we decided to include both wild-type strains as models for genome sequencing.

Assembly, annotation, and general features of the *B. methanolicus* MGA3 and PB1 genomes. The *B. methanolicus* MGA3 genome was sequenced with 20-fold coverage, and the direct outcome was 87 large contigs totally encoding about 3.4 Mb of DNA sequence. After manual gap filling using sequence alignments and PCR, the total number of large contigs was reduced to 12, including the previously described plasmid pBM19 (10) and the 69-kb plasmid pBM69 discovered here (see below). Nine contigs of 517 to 3,068 bp were found to appear in 2 to 15 near-identical copies mainly associated with genes encoding recombinases, transposases, and the 16S-23S-5S rRNA clusters. All attempts to experimentally close these remaining gaps failed due to highly repetitive

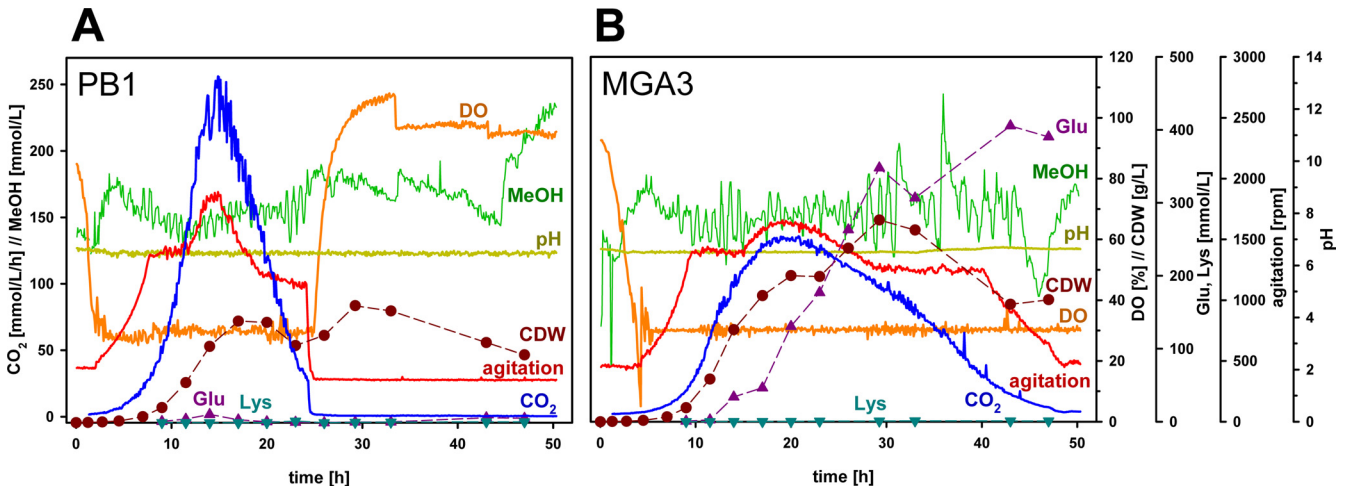

FIG 1 Summary of on-line and off-line analyses from fed-batch methanol cultivation of PB1 (A) and MGA3 (B) in UMN1 medium. CO_2, CO_2 evolution rate as a function of time (mmol liter^{-1} h^{-1}); CDW, dry weight (g liter^{-1}) of cells (filled circles), calculated from OD_{600} measurements by correlation to selected measurements of dry weights of cells; Glu, glutamate concentration in the medium (mmol liter^{-1}) (filled triangles); Lys, lysine concentration in the medium (mmol liter^{-1}) (filled inverted triangles); MeOH, methanol concentration (mmol liter^{-1}), determined by in-line mass spectrometric measurement in the exhaust gas and automatically held constant at 150 mmol liter^{-1}; DO, dissolved oxygen (%). Values for CO_2, dry weight of cells, Glu, and Lys are corrected for volume changes during cultivation.

DNA sequences in these regions. The average size of the 110 manually filled gaps was 251 bp, with the majority of the gap sequences being represented by the original 31 small contigs (101 to 449 bp), while the average length of new sequence was 79 bp. The size of the genome represented within the remaining 12 contigs is 3,398,992 bp (3,399 kb), and based on the average size of the manually filled gaps (249 bp), we estimated that this should represent at least 99.93% of the total MGA3 genome sequence.

The *B. methanolicus* PB1 genome was sequenced in 8-kb paired ends with 23-fold coverage, and the direct outcome from the Newbler assembly was 30 large contigs organized in 3 scaffolds, totally encoding about 3.4 Mb of DNA sequence. After manual gap filling using sequence alignments and PCR, the total number of large contigs was reduced to 4, including a pBM19-like plasmid (see below). In addition, 3 smaller contigs (contigs 5, 6, and 7, of 1,484 bp, 759 bp, and 304 bp, respectively), which had not been included in the original scaffolds and were not connected in the manual gap filling, were included in the final genome, since they were found to encode missing tRNA and rRNA genes organized in the same order as in the MGA3 strain. The size of the genome represented within the remaining 7 contigs is 3,426,513 bp (3,426 kb), and based on the average size of the manually filled gaps (123 bp), we estimate that this should represent at least 99.98% of the total PB1 genome sequence.

Both genome sequences were automatically annotated by using the services of JCVI (formerly TIGR), BASys (40), and PGAAP (from NCBI). In addition, genes of particular interest were all manually annotated using BLAST (2). The overall GC contents of both genomes were low, 38.5% (MGA3) and 39.0% (PB1), well below the GC contents of *Bacillus subtilis* and *Bacillus halodurans* (Table 1). Both the genome size and the number of open reading frames (ORF) were low compared to those of *B. subtilis*, and about 75% of all ORFs identified encoded proteins with annotated functions.

***B. methanolicus* plasmids.** In contrast to *B. subtilis* and *B. halodorans*, which carry no natural plasmids (Table 1), *B. methanolicus* strains harbor plasmids. The pivotal role of pBM19 for *B. methanolicus* MGA3 methylotrophy has been well documented by us (10, 26). We show here that the corresponding PB1 plasmid, designated pBM20, is 20 kb and contains *mdh* and RuMP pathway genes, analogously to pBM19. The phosphofructokinase gene of pBM20, *pfk*, contained a 2-nucleotide insertion leading to a frameshift mutation and a concomitant translational stop codon that should render this gene nonfunctional. This implies that this strain must recruit Pfk activity needed for the RuMP pathway

TABLE 1 Genome features of selected *Bacillus* spp.

Characteristic	*B. methanolicus*		*B. subtilis* 168	*B. halodurans* C-125
	MGA3	PB1		
No. of large contigs[a]	10 (+2)[b]	3 (+1)	1	1
No. of plasmids	2 (19 kb, 69 kb)	1 (20 kb)	0	0
Avg contig size (bp)	283,249	856,628		
Total size (bp)	3,398,992	3,426,513	4,215,606	4,202,353
GC content (%)	38.5	39.0	43	43
No. of predicted protein coding sequences	3,435	3,410	4,100	4,066
Status	Partially assembled	Partially assembled	Complete	Complete
GenBank accession no.	ADWW00000000	AFEU00000000	AL009126	BA000004

[a] >5 kb.
[b] Numbers in parentheses refer to the plasmids.

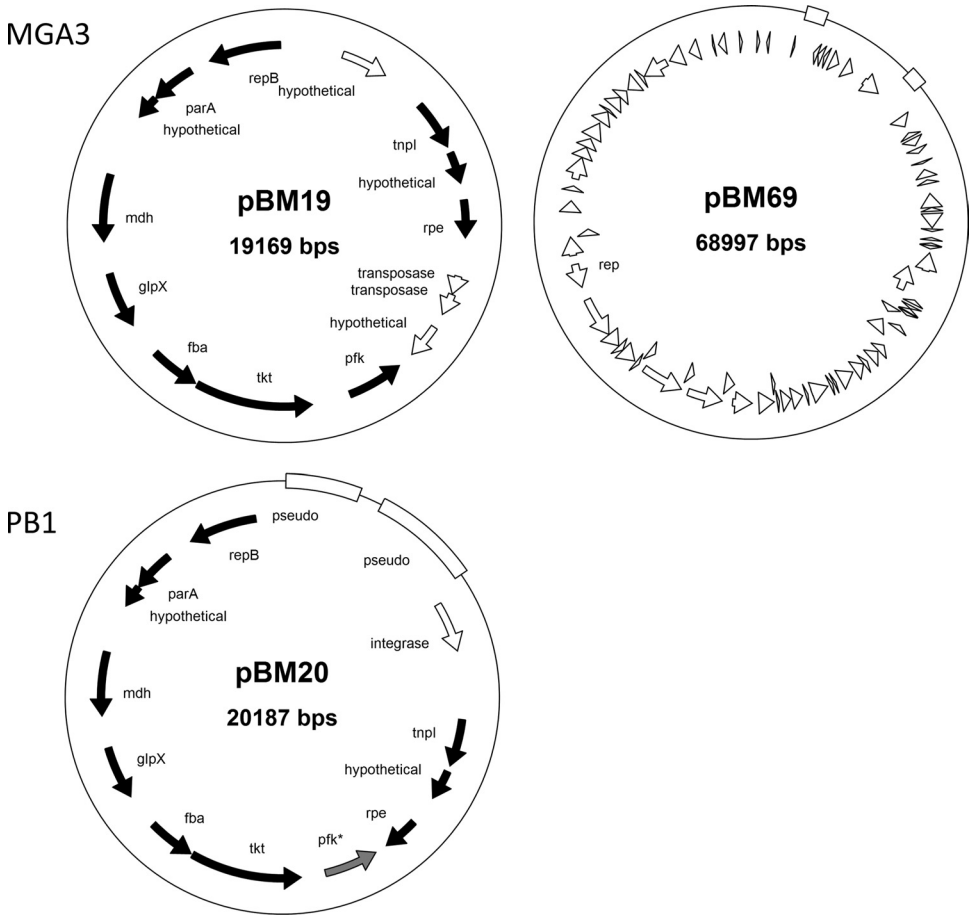

FIG 2 Physical maps of plasmids pBM19 and pBM69 from MGA3 and of plasmid pBM20 from PB1. Filled arrows show genes that are conserved between pBM19 and pBM20, while open arrows and boxes indicate coding regions that differ between the plasmids. The *pfk* gene in pBM20 is nonfunctional due to a frameshift mutation. For more detailed information about the coding sequences in pBM69, see GenBank accession code ADWW01000012 (locus tags MGA3_17472 to MGA3_17882). For the pBM19 and pBM20 genes, see the text.

from an alternative gene located on the chromosome (see below). We also noticed that pBM19 and pBM20 are somewhat different with respect to the remaining genes and their organization (Fig. 2). Nonetheless, the biological impact of these discrepancies remains unknown.

We also discovered that MGA3 has one additional, circular, 69-kb large plasmid designated pBM69, with 79 predicted coding sequences (CDSs), including a putative replication initiation protein gene. Its deduced gene product shared 52% overall primary sequence identity to the replication initiation protein of plasmid pBMB67 in *Bacillus thuringiensis* (13). The remaining CDSs of pBM69 encoded a number of hypothetical and unknown proteins with no assigned roles in cell metabolism. No plasmid analogous to pBM69 was identified in PB1, and the relevant CDSs were also not found on the PB1 chromosome.

***B. methanolicus* carries three *mdh* genes and one *act* gene.** The methanol dehydrogenase gene *mdh* was originally cloned and characterized from *B. methanolicus* strain C1 (21), and later we showed that the corresponding *mdh* gene of *B. methanolicus* MGA3 was located on plasmid pBM19 (10). Inspection of the MGA3 genome sequence unraveled two additional chromosomal genes, denoted *mdh2* and *mdh3*, both encoding putative MDH proteins. Still, only one chromosomal *act* gene, encoding the MDH activator protein (28), was found (Table 2). The deduced Mdh2 and Mdh3 proteins were 96% identical to each other, and they shared only 61% and 62% overall primary sequence identity to the pBM19-encoded Mdh protein.

Inspection of the PB1 genome sequence confirmed the presence of three methanol dehydrogenase genes, one located on pBM20 and two on the chromosome, and one chromosomal *act* gene (Table 2). The *mdh* gene located on pBM20 was 92% identical to the MGA3 *mdh* gene located on pBM19, and the respective deduced gene products displayed 93% primary sequence identity. One of the chromosomal PB1 genes, denoted *mdh1*, encoded an Mdh1 protein with 92% and 89% primary sequence identity to the PB1 and MGA3 Mdh proteins, respectively. The second chromosomal PB1 gene, denoted *mdh2*, encoded a putative Mdh2 protein with 91% and 92% primary sequence identity to the MGA3 Mdh2 and Mdh3 proteins, respectively, and only 59% and 60% identity to the PB1 Mdh and Mdh1 proteins, respectively. We are currently in the process of recombinant production, purification, and biochemical characterization of all six MDH proteins.

***B. methanolicus* encodes chromosomal homologues to all the RuMP pathway genes of pBM19 and pBM20.** Inspection of the *B. methanolicus* MGA3 genome sequence revealed a number of hitherto unknown, putative RuMP pathway genes (Table 2; Fig.

TABLE 2 Genes involved in methanol oxidation and concomitant formaldehyde metabolism in the *B. methanolicus* MGA3 genome sequence and their counterparts in PB1

Locus tag in MGA3	Locus tag in PB1	% Amino acid identity	Common name	Gene	EC no.	Localization[a]	Pathway[b]	Upregulated by methanol[c]
MGA3_17392	PB1_17533	93	Methanol dehydrogenase	*mdh*	1.1.1.244	pBM19	MO	Yes
	PB1_14569	89[d]	Methanol dehydrogenase 1	*mdh1*[d]	1.1.1.244			NA
MGA3_07340	PB1_12584[e]	91[e]	Methanol dehydrogenase 2	*mdh2*	1.1.1.244	C	MO	No
MGA3_10725			Methanol dehydrogenase 3	*mdh3*	1.1.1.244	C	MO	No
MGA3_09170	PB1_14394	97	Methanol dehydrogenase activator protein	*act*		C	MO	No
MGA3_15306	PB1_00480	98	3-Hexulose-6-phosphate synthase	*hps*	4.1.2.43	C	FA	Yes
MGA3_15301	PB1_00485	98	6-Phospho-3-hexuloisomerase	*phi*	5.3.1.27	C	FA	Yes
MGA3_17457			6-Phosphofructokinase	*pfk*	2.7.1.11	pBM19	FA	Yes
MGA3_03000	PB1_16819	96	6-Phosphofructokinase-2	*pfk2*	2.7.1.11	C	FA	No
MGA3_17377	PB1_17523	96	Fructose-bisphosphate aldolase	*fba*	4.1.2.13	pBM19	FA	Yes
MGA3_01355	PB1_07992	94	Fructose-bisphosphate aldolase-2	*fba2*	4.1.2.13	C	FA	No
MGA3_17462	PB1_17518	97	Transketolase	*tkt*	2.2.1.1	pBM19	FA	Yes
MGA3_15171	PB1_00595	94	Transketolase-2	*tkt2*	2.2.1.1	C	FA	No
MGA3_01350	PB1_07997	90	Transaldolase	*tal*	2.2.1.2	C	FA	No
MGA3_17382	PB1_17528	96	Fructose-bisphosphatase	*glpX*	3.1.3.11	pBM19	FA	Yes
MGA3_01340	PB1_08007	97	Fructose-bisphosphatase-2	*glpX2*	3.1.3.11	C	FA	No
MGA3_17437	PB1_17503	94	Ribulose-phosphate 3-epimerase	*rpe*	5.1.3.1	pBM19	FA	Yes
MGA3_14311			Ribulose-phosphate 3-epimerase-2	*rpe2*	5.1.3.1	C	FA	No
MGA3_01280	PB1_08082	95	Ribose 5-phosphate isomerase	*rpiB*	5.3.1.6	C	FA	No
MGA3_16421	PB1_10192	95	Glucose-6-phosphate isomerase	*pgi*	5.3.1.9	C	FOI	No
MGA3_09280	PB1_14524	94	Glucose-6-phosphate dehydrogenase	*zwf1*	1.1.1.49	C	FOI	ND
MGA3_15311	PB1_00475	91	Glucose-6-phosphate dehydrogenase	*zwf2*	1.1.1.49	C	FOI	Yes
MGA3_11305	PB1_04625	93	6-Phosphogluconolactonase	*pgl*	3.1.1.31	C	FOI	No
MGA3_09290	PB1_14534	96	6-Phosphogluconate dehydrogenase, decarboxylating	*gnd*	1.1.1.44	C	FOI	No
MGA3_09460	PB1_14689	88	5,10-Methylene-tetrahydrofolate dehydrogenase/5,10-methylene-tetrahydrofolate cyclohydrolase	*folD*	1.5.1.5/3.5.4.9	C	FOV	No
MGA3_08300	PB1_13509	94	Formate-tetrahydrofolate ligase	*fhs*	6.3.4.3	C	FOV	No
MGA3_06625	PB1_11719	94	Formate dehydrogenase, alpha chain	*fdhA*	1.2.1.2	C	FOV	No
MGA3_06630	PB1_11724	86	Formate dehydrogenase family accessory protein	*fdhD*		C	FOV	No

[a] C, chromosome.
[b] MO, methanol oxidation; FA, formaldehyde assimilation II (RuMP cycle); FOI, formaldehyde oxidation I (cyclic pentose phosphate pathway); FOV, formaldehyde oxidation V (tetrahydrofolate pathway).
[c] Yes or No, upregulated transcription or not upregulated transcription, respectively, on methanol versus mannitol in MGA3. NA, not analyzed; ND, not detectable.
[d] *mdh1* is found only in PB1 and is compared to the MGA3 *mdh* gene.
[e] The PB1 counterpart of *mdh2*/*mdh3* has been given the gene designation *mdh2* and is 92% identical to *mdh3*.

3). A *tal* gene encoding transaldolase was identified, suggesting that this bacterium has all the genes putatively representing both a fructose bisphosphate aldolase/seduheptulose bisphosphatase (FBPA/SBPase) variant (26) and a FBPA/transaldolase (TA) regeneration variant of the RuMP pathway (see reference 10). Whether both of these variants are biologically significant during the methylotrophic growth of *B. methanolicus* remains unknown. Moreover, a *rpiB* gene (encoding ribose-5-phosphate isomerase) was found, which likely represents the previously missing step of the RuMP pathway regeneration phase, the conversion of ribose-5-phosphate to ribulose-5-phosphate (10). The *rpiB* gene would play a role in the RuMP pathway irrespective of the variant of the regeneration phase being used. Homologues representing all five RuMP pathway genes located on pBM19 were found on the chromosome (*pfk2*, encoding 6-phosphofructokinase-2; *fba2*, encoding fructose-bisphosphate aldolase-2; *tkt2*, encoding transketolase-2; *glpX2*, encoding fructose bisphosphatase-2; *rpe2*, encoding ribulose-5-phosphate 3-epimerase-2). Taken together with *hps*, *phi*, *rpiB*, and possibly also *tal*, these findings imply that *B. methanolicus* has a complete assimilatory RuMP pathway solely encoded by chromosomal genes. The same observations overall were made in the PB1 genome sequence (Table 2), except that this strain has no chromosomal *rpe2* homologue, and pBM20 carries no functional *pfk* gene (see above).

***B. methanolicus* has genes representing both a cyclic dissimilatory RuMP pathway and a linear tetrahydrofolate pathway for formaldehyde dissimilation.** A linear dissimilatory pathway for formaldehyde oxidation via formate and to CO_2 in *B. methanolicus* MGA3 has been experimentally documented by using ^{13}C labeling experiments (35). This pathway was proposed to include formaldehyde dehydrogenase (FADH) and formate dehydrogenase (FDH) activities, as in *B. subtilis*. The *B. methanolicus* genome sequences contained no *fadh* gene. However, a putative *fdh* gene and a formate dehydrogenase family accessory protein gene, *fdhD*, were identified, as well as *folD* (encoding bifunctional methylene tetrahydrofolate dehydrogenase/methylene/methenyl tetrahydrofolate cyclohydrolase) and *fhs* (encoding formate tetrahydrofolate ligase) (Table 2). Together, these genes represent a putative linear

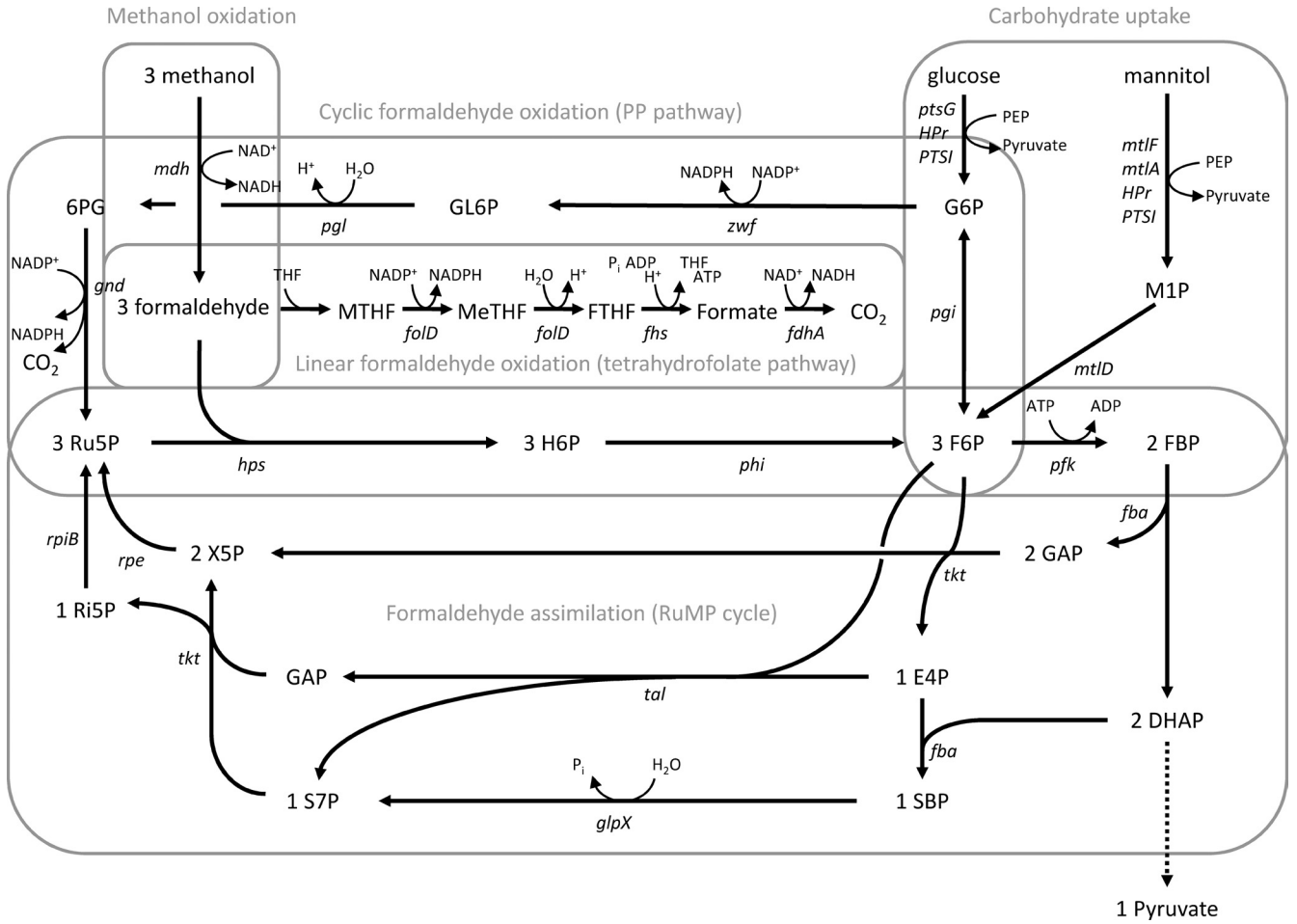

FIG 3 Proposed methylotrophic and important carbohydrate assimilation pathways in *B. methanolicus*. Genes: *mdh*, methanol dehydrogenase (EC 1.1.1.244); *hps*, 3-hexulose-6-phosphate synthase (EC 4.1.2.43); *phi*, 6-phospho-3-hexuloisomerase (EC 5.3.1.27); *pfk*, 6-phosphofructokinase, (EC 2.7.1.11); *fba*, fructose-bisphosphate aldolase (EC 4.1.2.13); *tkt*, transketolase (EC 2.2.1.1); *glpX*, fructose-bisphosphatase (EC 3.1.3.1); *tal*, transaldolase (EC 2.2.1.2); *rpe*, ribulose-phosphate 3-epimerase (EC 5.1.3.1); *rpiB*, ribose-5-phosphate isomerase (EC 5.3.1.6); *folD*, 5,10-methylene-tetrahydrofolate dehydrogenase/5,10-methenyl-tetrahydrofolate cyclohydrolase (EC 1.5.1.5/EC 3.5.4.9); *fhs*, formate-tetrahydrofolate ligase (EC 6.3.4.3); *fdhA*, formate dehydrogenase (EC 1.2.1.2); *pgi*, glucose-6-phosphate isomerase (EC 5.3.1.9); *zwf*, glucose-6-phosphate dehydrogenase (EC 1.1.1.49); *gnd*, 6-phosphogluconate dehydrogenase (EC 1.1.1.44); *pgl*, 6-phosphogluconolactonase (EC 3.1.1.31); *PTSI*, phosphoenolpyruvate–protein phosphotransferase (EC 2.7.3.9); *HPr*, phosphocarrier protein; *ptsG*, PTS-glucose-specific transporter subunit IICBA (EC 2.7.1.69); *mtlF*, mannitol-specific phosphotransferase enzyme IIA component (EC 2.7.1.69); *mtlA*, PTS system mannitol-specific enzyme IIBC component (EC 2.7.1.69); *mtlD*, mannitol-1-phosphate 5-dehydrogenase (EC 1.1.1.17). Metabolites: H6P, 3-hexulose 6-phosphate; F6P, fructose-6-phosphate; FBP, fructose-1,6-bisphosphate; GAP, glyceraldehyde 3-phosphate; DHAP, dihydroxyacetone phosphate; E4P, erythrose-4-phosphate; SBP, sedoheptulose-1,7-bisphosphate; S7P, sedoheptulose-7-phosphate; Ri5P, ribose-5-phosphate; X5P, xylulose-5-phosphate; Ru5P, ribulose-5-phosphate; MTHF, methylene tetrahydrofolate; MeTHF, methenyl tetrahydrofolate; FTHF, formate tetrahydrofolate; G6P, glucose-6-phosphate; GL6P, gluconolactone 6-phosphate; 6PG, 6-phosphogluconate; M1P, mannitol-1-phosphate.

dissimilatory tetrahydrofolate pathway for the oxidation of formaldehyde into CO_2 (see Fig. 3). Such pathways are widely distributed among methylotrophic bacteria, and in addition to playing a role in formaldehyde detoxification and energy generation, they are also important for providing C_1 units for biosynthetic reactions in the cells (41).

A set of genes, including *pgi* (encoding glucose-6-phosphate isomerase), *zwf1*, and *zwf2* (encoding glucose-6-phosphate dehydrogenases), *pgl* (encoding 6-phosphogluconolactonase), and *gnd* (encoding 6-phosphogluconate dehydrogenase), were found that should represent—together with *hps* and *phi*—an alternative cyclic dissimilatory RuMP pathway for the oxidation of formaldehyde into CO_2 and the regeneration of Ru5P (Fig. 3). This pathway is analogous to the oxidative pentose phosphate (PP) pathway widely distributed in bacteria. The *zwf2* gene was colocalized with *hps* and *phi* as a putative operon on the chromosome (see below), while *zwf1* was located elsewhere. The overall findings made here were similar in MGA3 and PB1 (Table 2), although the organization of the respective genes differed slightly. The cyclic dissimilatory RuMP pathway plays an important energetic role in generating reducing power [NAD(P)H], and it has been argued that it represents a substitute for the lack of a complete TCA cycle for such purposes in many methylotrophic bacteria (15).

Gene expression analysis of *B. methanolicus* MGA3 cells growing on methanol versus on mannitol. Our findings here imply that *B. methanolicus* MGA3 has chromosomal genes presumably constituting complete pathways for methanol oxidation

TABLE 3 Genes involved in mannitol and glucose uptake and metabolism

Locus tag in MGA3	Locus tag in PB1	% Amino acid identity	Common name	Gene	EC no.	Upregulated by mannitol[a]
MGA3_12915	PB1_06237	88	Mannitol-1-phosphate 5-dehydrogenase	*mtlD*	1.1.1.17	Yes
MGA3_12920	PB1_06242	97	Mannitol-specific phosphotransferase enzyme IIA component	*mtlF*	2.7.1.69	Yes
MGA3_12925	PB1_06247	88	Transcriptional regulator	*mtlR*		Yes
MGA3_12930	PB1_06252	93	PTS system mannitol-specific enzyme IIBC component	*mtlA*	2.7.1.69	Yes
MGA3_16763	PB1_05647	92	PTS-glucose-specific transporter subunit IICBA	*ptsG*	2.7.1.69	No
MGA3_16768	PB1_05652	88	BglG family transcriptional antiterminator	*glcT*		No
MGA3_09280	PB1_14524	94	Glucose-6-phosphate dehydrogenase	*zwf1*	1.1.1.49	ND
MGA3_15311	PB1_00475	91	Glucose-6-phosphate dehydrogenase	*zwf2*	1.1.1.49	No
MGA3_13541	PB1_02110	97	Phosphocarrier protein HPr	*hpr*		No
MGA3_13546	PB1_02105	90	PtsI—phosphoenolpyruvate-protein phosphotransferase	*ptsP*	2.7.3.9	No

[a] Yes or No, upregulated transcription or not upregulated transcription, respectively, on mannitol versus on methanol in MGA3. ND, Not detectable.

(*mdh2*, *mdh3*, and *act*), formaldehyde dissimilation (one linear tetrahydrofolate and one cyclic RuMP pathway), and formaldehyde assimilation (assimilatory RuMP pathway). We demonstrated previously that the pBM19-encoded RuMP pathway genes are transcriptionally upregulated in MGA3 cells growing on methanol (26), and it was of interest to extend our understanding regarding the regulation of gene expression upon methylotrophic versus nonmethylotrophic growth. Initially, we implemented a whole-genome gene expression microarray to compare the transcription levels of all genes in MGA3 cells growing on methanol versus on mannitol. In total, 102 genes were significantly upregulated in cells growing on methanol, while 64 genes were upregulated in cells growing on mannitol (for details, see http://www.ncbi.nlm.nih.gov/geo/query/acc.cgi?acc=GSE35298).

We then applied qPCR for targeted analyses of all genes with assigned putative roles in methanol consumption as listed in Table 2. In agreement with previous data, all five RuMP pathway genes positioned on pBM19 were transcriptionally upregulated by methanol (Table 2). In contrast, the transcription levels of the respective chromosomal homologues, as well as those of *rpiB* and *tal*, were not significantly affected by the carbon source. Taken together with the higher copy number of all pBM19 genes (10), it was tempting to assume that these chromosomal genes do not play important roles for methylotrophy in *B. methanolicus*. Considering that the *pfk* gene located on pBM20 in PB1 is inactive (see Fig. 2), it is plausible to believe that the overall regulation and role of RuMP pathway genes might be different in these two wild-type strains. The transcription level of *zwf2* was 3-fold upregulated in cells growing on methanol compared to that in cells growing on mannitol, indicating that this gene is cotranscribed and is accordingly coregulated as part of an operon together with the RuMP pathway genes *hps* and *phi*. In contrast, *zwf1* transcripts were hardly detectable under any growth conditions, suggesting that *zwf1* is a pseudogene with no biological function. The transcription levels of the remaining putative cyclic dissimilatory RuMP pathway genes *gnd*, *pgi*, and *pgl* were 2- to 3-fold lower in cells growing on methanol than in cells growing on mannitol. It should be kept in mind that these genes most likely play important roles in the generation of reducing power and energy in cells during growth on mannitol (see below). Transcription of the putative dissimilatory tetrahydrofolate pathway genes *folD*, *fhs*, *fdhA*, and *fdhD* was similar on methanol and mannitol, suggesting that these genes are important for cell metabolism under both growth conditions tested. In total there was good agreement between the qPCR data and the corresponding microarray data.

***B. methanolicus* mannitol and glucose uptake systems.** *B. methanolicus* strains can grow on few multicarbon sources, and they are therefore collectively designated restricted methylotrophs (11). Testing of MGA3 and PB1 for growth in minimal medium with a number of different C sources (20 g liter^{-1}) in this study revealed that both wild-type strains grew well on methanol, mannitol, and glucose, while they could not grow on maltose, raffinose, ribose, and sorbitol under the conditions tested. These results are somewhat different from those of previous reports stating that PB1 can grow on all the C sources mentioned above (4), and the reason for this discrepancy is unknown. The ability to grow rapidly on the alternative C source mannitol is a very important and useful trait, enabling the study of genetic regulation and physiology related to methylotrophy. In bacteria, mannitol and glucose enter the cells via mannitol-1-phosphate and glucose-6-phosphate, respectively, and are converted to fructose-6-phosphate, which can either be further metabolized via the Entner-Doudoroff pathway or, alternatively, oxidized via the PP pathway (Fig. 3). Gene clusters putatively involved in mannitol uptake and assimilation were identified in the *B. methanolicus* MGA3 and PB1 genomes (Table 3), including the genes *mtlD* (mannitol-1-phosphate 5-dehydrogenase), *mtlF* (mannitol-specific phosphotransferase [PTS] enzyme IIA component), *mtlR* (transcriptional regulator), and *mtlA* (mannitol-specific PTS enzyme IIBC component). These four genes are organized as an operon on the chromosome, as in *Geobacillus stearothermophilus* (GenBank accession no. BSU18943) (25) and similar to the pattern in *B. subtilis* (GenBank accession no. AL009126). Also, a *ptsG* gene putatively encoding a glucose uptake system was identified in both genome sequences (Table 3). The gene expression data (see above) showed that transcript levels of all the four mannitol uptake and assimilation genes are significantly higher in MGA3 cells growing on mannitol than in cells growing on methanol (Table 3). These data confirm that this gene cluster is active during growth on mannitol.

The anaplerotic node around PEP and pyruvate. Pyruvate and phosphoenol pyruvate (PEP) represent key precursor metabolites in all living cells, together with acetyl coenzyme A (acetyl-CoA), oxaloacetate (OAA), and α-ketoglutarate (1). The supply of these metabolites in the cells has a strong impact on the biotechnological production of amino acids and other useful compounds. For example, L-lysine overproduction relies on an efficient supply of the precursor metabolite OAA, while L-glutamate production relies on high entry of carbon into the TCA cycle. This implies that regulating the carbon flow at the anaplerotic node represented by PEP and pyruvate might be of crucial importance when the goal is

TABLE 4 Genes involved in the TCA cycle, glyoxylate shunt, and anaplerotic reactions

Locus tag in MGA3	Locus tag in PB1	% Amino acid identity	Common name	Gene	EC no.	Pathway[a]
MGA3_03025	PB1_16794	97	Citrate (Si)-synthase II	*citY*	2.3.3.1	TCA
MGA3_16693	PB1_00055	96	Aconitate hydratase	*acnA*	4.2.1.3	TCA
MGA3_03030	PB1_16789	97	Isocitrate dehydrogenase [NADP(+)]	*icd*	1.1.1.42	TCA
MGA3_06345	PB1_11459	83	Dihydrolipoyllysine-residue succinyltransferase	*odhB*	2.3.1.61	TCA
MGA3_06350	PB1_11464	89	Oxoglutarate dehydrogenase (succinyl transferring)	*odhA*	1.2.4.2	TCA
MGA3_14936	PB1_00700	94	2-Oxoglutarate synthase, alpha subunit	*korA*	1.2.7.3	TCA
MGA3_14941	PB1_00695	96	2-Oxoglutarate synthase, beta subunit	*korB*	1.2.7.3	TCA
MGA3_14471	PB1_01175	98	Succinyl-CoA synthetase, subunit beta	*sucC*	6.2.1.5	TCA
MGA3_14476	PB1_01170	97	Succinyl-CoA synthetase, subunit alpha	*sucD*	6.2.1.5	TCA
MGA3_03260	PB1_16529	96	Succinate dehydrogenase, cytochrome b_{558} subunit	*sdhC*	1.3.99.1	TCA
MGA3_03265	PB1_16524	96	Succinate dehydrogenase, flavoprotein subunit	*sdhA*	1.3.99.1	TCA
MGA3_03270	PB1_16519	98	Succinate dehydrogenase, iron-sulfur subunit	*sdhB*	1.3.99.1	TCA
MGA3_04115	PB1_03575	92	Fumarate hydratase, class II	*fumC*	4.2.1.2	TCA
MGA3_10765	PB1_04250	94	Fumarate hydratase, class I	*fumA*	4.2.1.2	TCA
MGA3_03035	PB1_16784	94	Malate dehydrogenase	*citH*	1.1.1.37	TCA
MGA3_12305	PB1_05300	95	Malate:quinone oxidoreductase	*mqo*	1.1.5.4	TCA
MGA3_12485	PB1_05532	97	Isocitrate lyase	*aceA*	4.1.3.1	GxS
MGA3_12490	PB1_05537	95	Malate synthase	*aceB*	2.3.3.9	GxS
MGA3_13826	PB1_01810	96	Pyruvate carboxylase	*pyc*	6.4.1.1	AN
MGA3_08600	PB1_13864	94	Aspartate transaminase	*aspB*	2.6.1.1	AN
MGA3_09380	PB1_14609	90	Dihydrolipoyl dehydrogenase (E3)	*bfmbC*	1.8.1.4	AN
MGA3_13696	PB1_01955	94	Pyruvate dehydrogenase (acetyl transferring) (E1), α subunit	*pdhA*	1.2.4.1	AN
MGA3_13701	PB1_01950	98	Pyruvate dehydrogenase (acetyl transferring) (E1), β subunit	*pdhB*	1.2.4.1	AN
MGA3_13706	PB1_01945	86	Dihydrolipoyllysine-residue acetyltransferase (E2)	*pdhC*	2.3.1.12	AN
MGA3_13711	PB1_01940	95	Dihydrolipoyl dehydrogenase (E3)	*pdhD*	1.8.1.4	AN
MGA3_08930	PB1_14164	96	Glutamate dehydrogenase (NAD^+)	*yweB*	1.4.1.2	AN
MGA3_09355	PB1_14584	96	Methylmalonyl-CoA mutase, large subunit	*mutB*	5.4.99.2	AN
MGA3_01385	PB1_07957	94	Methylmalonyl-CoA mutase, large subunit	*mutB2*	5.4.99.2	AN
MGA3_09360	PB1_14589	85	Methylmalonyl-CoA mutase, small subunit	*mutA*	5.4.99.2	AN
MGA3_02480	PB1_17299	96	Phosphoenolpyruvate carboxykinase (ATP)	*pckA*	4.1.1.49	AN
MGA3_02925	PB1_16924	96	Alanine dehydrogenase	*ald*	1.4.1.1	AN

[a] Determined by the ExPASy Proteomics Server (http://expasy.org/). TCA, tricarboxylic acid cycle; GxS, glyoxylate shunt; AN, anaplerotic.

to overproduce either L-lysine or L-glutamate. Inspection of the MGA3 and PB1 genome sequences confirmed that *B. methanolicus* has one single pyruvate carboxylase (PC)-encoding gene represented by the recently cloned *pyc* gene of MGA3 (9) and one putative PEP carboxykinase gene (*pckA*), but no PEP carboxylase gene. We also identified the *pdhA* and *pdhB* genes putatively encoding the large and small subunits, respectively, of pyruvate dehydrogenase (Pdh) (Table 4). For example, we believe that the reduced L-glutamate production in MGA3 cells upon PC overexpression (9) implies that there is an imbalance in the concentrations of OAA versus acetyl-CoA, eventually resulting in reduced entry of PEP and pyruvate into the TCA cycle. Possibly, *pdhA* and *pdhB* may represent two additional targets, together with *pyc*, to redirect and control carbon flow at this point. Moreover, alanine dehydrogenase can convert pyruvate into the amino acid L-alanine, thus representing an alternative route. *B. methanolicus* MGA3 cells produce substantial levels of this amino acid (13 g $liter^{-1}$) in fed-batch methanol cultivation (9), and the *ald* gene (Table 4) might therefore represent another mutational target to maximize carbon flow from pyruvate toward L-lysine or L-glutamate.

***B. methanolicus* has genes representing a complete TCA cycle and a glyoxylate shunt, but no ethylmalonyl-CoA pathway.** It is well known that many methylotrophic bacteria lack a complete TCA cycle and that the formaldehyde assimilatory and dissimilatory routes play major roles in the generation of energy and reducing power (15). Some methylotrophs also lack a glyoxylate shunt for acetyl-CoA assimilation but instead possess an alternative ethylmalonyl-CoA pathway for such purposes (1, 34). *B. methanolicus* MGA3 cells presumably have a high entry of methanol-derived carbon into the first three steps of the TCA cycle catalyzed by citrate synthase (CS), aconitate hydratase (Acn), and isocitrate dehydrogenase (Icd), leading to the generation of α-ketoglutarate. A substantial portion of this precursor metabolite is then directly converted to L-glutamate (9, 12). Together with the lack of any significant 2-oxoglutarate dehydrogenase (OGDH) activity in cell extracts (12), this has led to the assumption that *B. methanolicus* also lacks a complete TCA cycle. However, genes representing all biochemical steps of a complete TCA cycle were identified in both *B. methanolicus* genomes, including the *odhAB* operon encoding a putative OGDH enzyme (Table 4). *B. subtilis* encodes two CS genes, but we identified only one CS gene, *citY*, in both *B. methanolicus* strains MGA3 and PB1. We demonstrated previously that *citY* encoded an active CSII protein, and a frameshift mutation in this gene resulted in dramatically reduced L-glutamate production in a MGA3 genetic background (12).

TABLE 5 Genes involved in glutamate synthesis and metabolism

Locus tag in MGA3	Locus tag in PB1	% Amino acid identity	Common name	Gene	EC no.
MGA3_02745	PB1_17089	95	Carbon catabolite repression transcriptional regulator	*ccpA*	
MGA3_06010	PB1_11134	90	Glutaminase	*glsA*	3.5.1.2
MGA3_08135	PB1_13334	85	Transcriptional activator of arginine utilization operons	*rocR*	
MGA3_08930	PB1_14164	96	Glutamate dehydrogenase	*yweB*	1.4.1.2
MGA3_09430	PB1_14659	98	Arginine repressor	*ahrC*	
MGA3_10580	PB1_03940	92	Glutamate synthase (NADPH)	*gltA2*	1.4.1.13
MGA3_11185	PB1_04590	93	Transcriptional pleiotropic regulator involved in global nitrogen regulation	*tnrA*	
MGA3_12495	PB1_05542	96	1-Pyrroline-5-carboxylate dehydrogenase	*rocA*	1.5.1.12
MGA3_12285	PB1_05275	96	Glutamate synthase (NADPH)	*gltB*	1.4.1.13
MGA3_12290	PB1_05280	96	Glutamate synthase (NADPH)	*gltA*	1.4.1.13
MGA3_12295	PB1_05285	96	Transcriptional activator of the glutamate synthase operon	*gltC*	
MGA3_13010	PB1_06417	97	Arginase	*rocF*	3.5.3.1
MGA3_14511	PB1_01135	99	Transcriptional pleiotropic repressor	*codY*	
MGA3_15006	PB1_00630	94	Transcriptional repressor of glutamine synthetase	*glnR*	
MGA3_15011	PB1_00625	98	Glutamine synthetase, type I	*glnA*	6.3.1.2
MGA3_16406	PB1_10177	92	Ornithine aminotransferase	*rocD*	2.6.1.13

Genes representing a glyoxylate cycle, *aceA* and *aceB*, encoding isocitrate lyase and malate synthase, respectively, were also found, while no genes representing any ethylmalonyl-CoA pathway were identified. The latter pathway was recently documented in the Gram-negative methylotroph *Methylobacterium extorquens* AM1 (1, 34), and to our knowledge, no analogous pathways have been identified in any Gram-positive methylotrophic bacterium.

Genes and regulators putatively involved in L-glutamate biosynthesis. The biosynthesis of L-glutamate represents a major part of cellular metabolism linking carbon metabolism and nitrogen metabolism. Also included here are the biosynthetic pathways for the amino acids L-glutamine and L-arginine. In contrast to the closely related *B. subtilis*, *B. methanolicus* MGA3 synthesizes and secretes large amounts of L-glutamate, and it was of interest to explore whether this difference can be directly attributed to the genes and regulators involved in L-glutamate metabolism. In *B. subtilis*, the central enzymes involved are glutamate synthase (GOGAT; encoded by the *gltAB* operon), two different glutamate dehydrogenases (GDH; encoded by *rocG* and *gudB*), and glutamine synthetase (GS; encoded by *glnA*). In this bacterium, L-glutamate is reported to be synthesized exclusively by the reductive amination of α-ketoglutarate catalyzed by GOGAT, and mutants deficient in this enzyme are L-glutamate auxotrophs (17). GDH, on the other hand, is only devoted to glutamate catabolism into α-ketoglutarate and further degradation in the TCA cycle by OGDH. Overexpression of *rocG* in *B. subtilis* resulted in an ability to grow on L-glutamate (17). L-Glutamate can be aminated to L-glutamine, catalyzed by GS (17).

Putative *B. methanolicus* genes involved in L-glutamate metabolism are listed in Table 5. In contrast to *B. subtilis*, which has two GDH genes, *rocG* and *gudB*, *B. methanolicus* has only one GDH gene, *yweB*. *B. methanolicus* has a *gltAB* operon putatively encoding a GOGAT similar to that reported for *B. subtilis* (7), and it has one additional *gltA2* gene located elsewhere on the chromosome. One putative GS gene, *glnA*, was also identified and is analogous to a corresponding gene in *B. subtilis*. The MGA3 and PB1 genome sequences were similar with respect to all these genes, and still these two strains are very different with respect to L-glutamate production levels in fed-batch methanol cultivation (see above). Biochemical characterization and regulation of all these gene products are in progress in our research group, and this work will provide new insight into L-glutamate biosynthesis in *B. methanolicus* strains.

In *Corynebacterium glutamicum*, it has been reported that the *NCgl1221* gene encodes an active L-glutamate exporter (33, 42). Putative counterparts to this gene, originally annotated as a small-conductance mechanosensitive channel, were found in the MGA3 and PB1 genomes (locus tags MGA3_01925 and PB1_07357, here annotated as mechanosensitive ion channel family proteins). The *B. methanolicus* genes are considerably shorter than *NClg1221*, and the primary sequences of the deduced *B. methanolicus* gene products are 93% identical to each other and about 28% identical to the NClg1221 gene product. Whether these genes play any role in L-glutamate secretion in *B. methanolicus* remains to be experimentally tested.

L-Glutamate metabolism in *B. subtilis* is tightly controlled, and several transcriptional regulators are involved. Transcription of the *gltAB* operon is repressed by the global regulator TnrA in the absence of ammonium, while GltC activates *gltAB* transcription in the presence of sugars and in the absence of arginine. Transcription of *rocG* is subject to carbon catabolite repression exerted by CcpA in the presence of arginine, and *rocG* transcription is mediated by the activators RocR and AhrC. The *gudB* gene, on the other hand, is constitutively expressed in *B. subtilis*. Moreover, the global transcriptional regulators CodY and GlnR play important roles in regulating nitrogen metabolism in *B. subtilis* (16). GS, in addition to being feedback regulated, also plays a role in regulating the activity of the transcription factors GlnR and TnrA. Genes putatively encoding all the assumed important transcriptional regulators AhrC, CcpA, CodY, GlnR, GltC, RocR, and TnrA were also identified in the *B. methanolicus* MGA3 and PB1 genome sequences (Table 5). The role and impact of these regulatory genes for controlling L-glutamate and nitrogen metabolism in *B. methanolicus* remain to be tested experimentally.

***B. methanolicus* presumably uses the acetylase variant of the L-lysine biosynthetic pathway.** Some *B. methanolicus* genes en-

TABLE 6 Genes involved in the aspartate pathway

Step	Locus tag in MGA3	Locus tag in PB1	% Amino acid identity	Common name	Gene	EC no.
−1	MGA3_08600	PB1_13864	94	Aspartate transaminase	*aspB*	2.6.1.1
1	MGA3_14816	PB1_00835	95	Aspartate kinase I	*dapG*	2.7.2.4
1	MGA3_03250	PB1_16544	91	Aspartate kinase II	*lysC*	2.7.2.4
1	MGA3_06765	PB1_11794	92	Aspartate kinase III	*yclM*	2.7.2.4
2	MGA3_14811	PB1_00840	92	Aspartate-semialdehyde dehydrogenase	*asd*	1.2.1.11
3	MGA3_14821	PB1_00830	95	Dihydrodipicolinate synthase	*dapA*	4.2.1.52
4	MGA3_08665	PB1_13924	95	Dihydrodipicolinate reductase	*dapB*	1.3.1.26
5	MGA3_13651	PB1_02000	95	Tetrahydrodipicolinate *N*-acetyltransferase	*dapH*	2.3.1.89
6	MGA3_13566	PB1_02085	89	Acetyl-diaminopimelate aminotransferase	*patA*	2.6.1.-
7	MGA3_13656	PB1_01995	90	*N*-Acetyl-diaminopimelate deacetylase	*dapL*	3.5.1.47
8	MGA3_07875	PB1_13099	88	Diaminopimelate epimerase	*dapF*	5.1.1.7
9	MGA3_09090	PB1_14319	92	Diaminopimelate decarboxylase	*lysA*	4.1.1.20
10	MGA3_07720	PB1_05235	62	Putative L-lysine exporter	*lysE*	
10		PB1_00380		Putative L-lysine exporter	*lysE2*	
3a	MGA3_16241	PB1_10002	95	Homoserine dehydrogenase 1	*hom1*[a]	1.1.1.3
3a	MGA3_11045			Homoserine dehydrogenase 2	*hom2*	1.1.1.3
3b	MGA3_16251	PB1_10012	93	Homoserine kinase	*thrB*	2.7.1.39
3c	MGA3_16246	PB1_10007	96	Threonine synthase	*thrC*	4.2.3.1
4a	MGA3_14801	PB1_00850	94	Dipicolinate synthase, subunit A	*dpaA*	
4a	MGA3_14806	PB1_00845	95	Dipicolinate synthase, subunit B	*dpaB*	

[a] Only one *hom* gene is found in PB1.

coding enzymes of the aspartate pathway have previously been cloned and characterized, including *lysA* (encoding diaminopimelate decarboxylase [LysA]) (31), the three aspartokinase (AK) genes *dapG* (AKI), *lysC* (AKII), and *yclM* (AKIII) (27, 39), and *hom1* and *hom2* (encoding homoserine dehydrogenase [HD I and II, respectively]) (9). The *asd* (encoding aspartate-semialdehyde dehydrogenase) and *dapA* (encoding dihydrodipicolinate synthase) genes were also cloned by us (27), and we recently demonstrated that they both encode active enzymes (32). Overexpression of *dapG*, *lysC*, and *yclM* increased L-lysine production in wild-type *B. methanolicus* MGA3 up to 60-fold (corresponding to 11 g liter^{-1}) in fed-batch methanol cultivation (27), and we showed that *hom1* is the major target for *S*-(2-aminoethyl)-L-cysteine (AEC) resistance in *B. methanolicus* (9). The *B. methanolicus* genome sequences provided the remaining genes representing a complete aspartate pathway (Table 6). In particular, the finding of *dapH* (encoding tetrahydrodipicolinate *N*-acetyltransferase), *patA* (encoding acetyl-diaminopimelate aminotransferase), and *dapL* (encoding *N*-acetyl-diaminopimelate deacetylase) indicates that this organism uses the acetylase variant of the L-lysine biosynthetic pathway, as previously proposed by us (11). The *dapH* and *dapL* genes are colocalized as an operon. Also, the *asd*, *dapG*, and *dapA* genes are localized as a *dap* operon, together with *dpaA* and *dpaB* (encoding dipicolinate synthase subunits A and B, respectively) and presumably under coordinated transcriptional control, analogous to the situation in *B. subtilis*. The two L-threonine pathway genes *thrB* (encoding homoserine kinase) and *thrC* (encoding homoserine synthase) are also localized as an operon together with *hom1*. PB1 has no *hom2* gene, and the biological impact of this remains unknown.

L-Lysine export in *B. methanolicus* strains. A putative lysine exporter gene, *lysE*, was identified in the MGA3 genome, and the deduced LysE primary sequence showed highest similarity (53%) to the *yisU* gene-encoded protein from *B. subtilis* 168, annotated as a not yet characterized putative lysine exporter (36). Both the YisU and LysE amino acid sequences shared only a low similarity of 20% with the *C. glutamicum* LysE^{Cg} primary sequence. In contrast to *C. glutamicum* (8), no putative regulator genes were found associated with any of the putative lysine exporter genes in the *B. methanolicus* strains. Genome mining revealed two putative lysine exporter genes in the PB1 genome sequence, denoted *lysE* and *lysE2*, and the deduced amino acid sequences of the respective gene products share 20% identity with each other. The deduced LysE protein of MGA3 shared 62% and 44% primary sequence identity to the deduced LysE and LysE2 proteins of PB1, respectively. We are currently in the process of investigating the biological function and roles of all these genes for L-lysine export in *B. methanolicus* strains.

Concluding remarks. The first genome sequencing of bacteria belonging to thermotolerant bacilli is presented. Our results include a genomewide comparison between two *Bacillus methanolicus* wild-type strains, MGA3 and PB1, as well as a comparison of this species with other nonmethylotrophic bacilli. MGA3 and PB1 displayed major physiological differences in fed-batch methanol cultivation, and together these two strains represent a valuable model system for understanding plasmid-dependent methylotrophy. The differences in methanol consumption and respiration rate between these two strains were accompanied by different organization of the methanol dehydrogenase genes and of certain RuMP pathway genes. Our results open up possibilities for systems-level metabolic engineering of *B. methanolicus* for the overproduction of amino acids and other useful compounds from methanol. For example, PB1 produced very little L-glutamate compared to MGA3, and this could not be explained genetically. Ongoing analyses of the regulation and biochemistry of L-glutamate biosynthesis genes and enzymes should provide new insight into key bottlenecks for L-glutamate overproduction from methanol by *B. methanolicus*.

ACKNOWLEDGMENTS

This work was supported by a research grant from The Research Council of Norway.

We thank Bård Karsten Gustavsen and Lihua Yu for valuable contributions during the MGA3 genome gap-filling process and Roman Netzer for extracting the *B. methanolicus* genomic DNA and for valuable discussions. We also thank Ave Tooming-Klunderud at the Norwegian High-Throughput Sequencing Centre for valuable discussions during the PB1 assembly process.

REFERENCES

1. **Alber BE.** 2011. Biotechnological potential of the ethylmalonyl-CoA pathway. Appl. Microbiol. Biotechnol. **89**:17–25.
2. **Altschul SF, et al.** 1997. Gapped BLAST and PSI-BLAST: a new generation of protein database search programs. Nucleic Acids Res. **25**:3389–3402.
3. **Anthony C.** 1982. The biochemistry of methylotrophs. Academic Press, London, United Kingdom.
4. **Arfman N, et al.** 1992. Environmental regulation of alcohol metabolism in thermotolerant methylotrophic *Bacillus* strains. Arch. Microbiol. **157**: 272–278.
5. **Arfman N, et al.** 1997. Properties of an NAD(H)-containing methanol dehydrogenase and its activator protein from *Bacillus methanolicus*. Eur. J. Biochem. **244**:426–433.
6. **Aziz RK, et al.** 2008. The RAST Server: rapid annotations using subsystems technology. BMC Genomics **9**:75. doi:10.1186/1471-2164-9-75.
7. **Belitsky BR.** 2002. Biosynthesis of amino acids of the glutamate and aspartate families, alanine, and polyamines, p 203–231. *In* Sonenshein AL, Hoch JA, Losick L (ed), *Bacillus subtilis* and its closest relatives: from genes to cells. American Society for Microbiology, Washington, DC.
8. **Bellmann A, et al.** 2001. Expression control and specificity of the basic amino acid exporter LysE of *Corynebacterium glutamicum*. Microbiology **147**:1765–1774.
9. **Brautaset T, et al.** 2010. *Bacillus methanolicus* pyruvate carboxylase and homoserine dehydrogenase I and II and their roles for L-lysine production from methanol at 50 degrees C. Appl. Microbiol. Biotechnol. **87**:951–964.
10. **Brautaset T, Jakobsen M, Flickinger MC, Valla S, Ellingsen TE.** 2004. Plasmid-dependent methylotrophy in thermotolerant *Bacillus methanolicus*. J. Bacteriol. **186**:1229–1238.
11. **Brautaset T, Jakobsen M, Josefsen KD, Flickinger MC, Ellingsen TE.** 2007. *Bacillus methanolicus*: a candidate for industrial production of amino acids from methanol at 50 degrees C. Appl. Microbiol. Biotechnol. **74**:22–34.
12. **Brautaset T, et al.** 2003. Role of the *Bacillus methanolicus* citrate synthase II gene, *citY*, in regulating the secretion of glutamate in L-lysine-secreting mutants. Appl. Environ. Microbiol. **69**:3986–3995.
13. **Chao L, et al.** 2007. Complete nucleotide sequence of pBMB67, a 67-kb plasmid from *Bacillus thuringiensis* strain YBT-1520. Plasmid **57**:44–54.
14. **Chistoserdova L.** 2011. Modularity of methylotrophy, revisited. Environ. Microbiol. **13**:2603–2622.
15. **Chistoserdova L, Kalyuzhnaya MG, Lidstrom ME.** 2009. The expanding world of methylotrophic metabolism. Annu. Rev. Microbiol. **63**:477–499.
16. **Commichau FM, Forchhammer K, Stülke J.** 2006. Regulatory links between carbon and nitrogen metabolism. Curr. Opin. Microbiol. **9**:167–172.
17. **Commichau FM, Gunka K, Landmann JJ, Stülke J.** 2008. Glutamate metabolism in *Bacillus subtilis*: gene expression and enzyme activities evolved to avoid futile cycles and to allow rapid responses to perturbations of the system. J. Bacteriol. **190**:3557–3564.
18. **de Vries GE, Arfman N, Terpstra P, Dijkhuizen L.** 1992. Cloning, expression, and sequence analysis of the *Bacillus methanolicus* C1 methanol dehydrogenase gene. J. Bacteriol. **174**:5346–5353.
19. **de Vries GE, Kües U, Stahl U.** 1990. Physiology and genetics of methylotrophic bacteria. FEMS Microbiol. Rev. **6**:57–101.
20. **Dijkhuizen L, et al.** 1988. Isolation and initial characterization of thermotolerant methylotrophic *Bacillus* strains. FEMs Microbiol. Lett. **52**: 209–214.
21. **Dijkhuizen L, Levering PR, De Vries GE.** 1992. The physiology and biochemistry of aerobic methanol-utilizing Gram-negative and Gram-positive bacteria, p 149–181. *In* Murrel JC, Dalton H (ed), Methane and methanol utilizers. Plenum Press, New York, NY.
22. **Hanson RS, Dillingham R, Olson P.** 1996. Production of L-lysine and some other amino acids by mutants of *B. methanolicus*, p 227–236. *In* Lindstrom ME, Tabita FR (ed), Microbial growth on C_1 compounds. Kluwer Academic Publishers, Dordrecht, Netherlands.
23. **Heid CA, Stevens J, Livak KJ, Williams PM.** 1996. Real time quantitative PCR. Genome Res. **6**:986–994.
24. **Hektor HJ, Kloosterman H, Dijkhuizen L.** 2002. Identification of a magnesium-dependent NAD(P)(H)-binding domain in the nicotinoprotein methanol dehydrogenase from *Bacillus methanolicus*. J. Biol. Chem. **277**:46966–46973.
25. **Henstra SA, Tolner B, Duurkens RHT, Konings WN, Robillard GT.** 1996. Cloning, expression, and isolation of the mannitol transport protein from the thermophilic bacterium *Bacillus stearothermophilus*. J. Bacteriol. **178**:5586–5591.
26. **Jakobsen ØM, et al.** 2006. Upregulated transcription of plasmid and chromosomal ribulose monophosphate pathway genes is critical for methanol assimilation rate and methanol tolerance in the methylotrophic bacterium *Bacillus methanolicus*. J. Bacteriol. **188**:3063–3072.
27. **Jakobsen ØM, et al.** 2009. Overexpression of wild-type aspartokinase increases L-lysine production in the thermotolerant methylotrophic bacterium *Bacillus methanolicus*. Appl. Environ. Microbiol. **75**:652–661.
28. **Kloosterman H, Vrijbloed JW, Dijkhuizen L.** 2002. Molecular, biochemical, and functional characterization of a Nudix hydrolase protein that stimulates the activity of a nicotinoprotein alcohol dehydrogenase. J. Biol. Chem. **277**:34785–34792.
29. **Komives CF, Cheung LY, Pluschkell SB, Flickinger MC.** 2005. Growth of *Bacillus methanolicus* in seawater-based media. J. Ind. Microbiol. Biotechnol. **32**:61–66.
30. **Livak KJ.** 1997. Comparative C_T method. User bulletin no. 2. PE Applied Biosystems, Foster City, CA.
31. **Mills DA, Flickinger MC.** 1993. Cloning and sequence analysis of the meso-diaminopimelate decarboxylase gene from *Bacillus methanolicus* MGA3 and comparison to other decarboxylase genes. Appl. Environ. Microbiol. **59**:2927–2937.
32. **Nærdal I, Netzer R, Ellingsen TE, Brautaset T.** 2011. Analysis and manipulation of aspartate pathway genes for L-lysine overproduction from methanol by *Bacillus methanolicus*. Appl. Environ. Microbiol. **77**: 6020–6026.
33. **Nakamura J, Hirano S, Ito H, Wachi M.** 2007. Mutations of the *Corynebacterium glutamicum* NCgl1221 gene, encoding a mechanosensitive channel homolog, induce L-glutamic acid production. Appl. Environ. Microbiol. **73**:4491–4498.
34. **Peyraud R, et al.** 2009. Demonstration of the ethylmalonyl-CoA pathway by using ^{13}C metabolomics. Proc. Natl. Acad. Sci. U. S. A. **106**:4846–4851.
35. **Pluschkell SB, Flickinger MC.** 2002. Dissimilation of [^{13}C]methanol by continuous cultures of *Bacillus methanolicus* MGA3 at 50 degrees C studied by ^{13}C NMR and isotope-ratio mass spectrometry. Microbiology **148**: 3223–3233.
36. **Saier MH, et al.** 2002. Transport capabilities encoded within the *Bacillus subtilis* genome. J. Mol. Microbiol. Biotechnol. **4**:37–67.
37. **Sambrook J, Russell DW.** 2001. Molecular cloning: a laboratory manual, 3rd ed. Cold Spring Harbor Laboratory Press, Cold Spring Harbor, NY.
38. **Schendel FJ, Bremmon CE, Flickinger MC, Guettler M, Hanson RS.** 1990. L-Lysine production at 50 degrees C by mutants of a newly isolated and characterized methylotrophic *Bacillus* sp. Appl. Environ. Microbiol. **56**:963–970.
39. **Schendel FJ, Flickinger MC.** 1992. Cloning and nucleotide sequence of the gene coding for aspartokinase II from a thermophilic methylotrophic *Bacillus* sp. Appl. Environ. Microbiol. **58**:2806–2814.
40. **Van Domselaar GH, et al.** 2005. BASys: a web server for automated bacterial genome annotation. Nucleic Acids Res. **33**:W455–W459.
41. **Vorholt JA.** 2002. Cofactor-dependent pathways of formaldehyde oxidation in methylotrophic bacteria. Arch. Microbiol. **178**:239–249.
42. **Yao W, et al.** 2009. Expression and localization of the *Corynebacterium glutamicum* NCgl1221 protein encoding an L-glutamic acid exporter. Microbiol. Res. **164**:680–687.